Unsteady Transonic Small-Disturbance Theory Including Entropy and Vorticity Effects

John T. Batina*
NASA Langley Research Center, Hampton, Virginia

Modifications to unsteady transonic small-disturbance theory to include entropy and vorticity effects are presented. The modifications have been implemented in the computational aeroelasticity program-transonic small disturbance (CAP-TSD) code developed recently for aeroelastic analysis of complete aircraft configurations in the flutter critical transonic speed range. Entropy and vorticity effects have been incorporated within the solution procedure to analyze flows with strong shock waves more accurately. The modified code includes these effects while retaining the relative simplicity and cost efficiency of the TSD formulation. The paper presents detailed descriptions of the entropy and vorticity modifications along with calculated results and comparisons that assess the modified theory. These results are in good agreement with parallel Euler calculations and with experimental data. Therefore, the present method now provides the aeroelastician with an affordable capability to analyze relatively difficult transonic flows without having to solve the computationally more expensive Euler equations.

Nomenclature

C_p = pressure coefficient
C_{p^*} = critical pressure coefficient
ΔC_p = unsteady lifting pressure coefficient normalized by oscillation amplitude
c = airfoil chord
c_r = reference chord
c_v = specific heat at constant volume
f = function defining position of lifting surface
k = reduced frequency, $\omega c_r/2U$
M = freestream Mach number
s = change in entropy from freestream value
t = time, nondimensionalized by freestream speed and reference chord, U/c_r
Δt = nondimensional time step
U = freestream speed
x,y,z = nondimensional coordinates in streamwise, spanwise, and vertical directions, respectively
α = instantaneous angle of attack
α_0 = mean angle of attack
α_1 = amplitude of pitch oscillation
γ = ratio of specific heats
Γ = circulation
$\bar{\eta}$ = fractional semispan
σ = relaxation parameter
τ = nondimensional time, $2U/c_r$
ϕ = disturbance velocity potential, nondimensionalized by freestream speed and reference chord
ω = angular frequency

Introduction

CONSIDERABLE progress has been made over the past decade on developing methods for aeroelastic analysis in the flutter critical transonic speed range.[1] Much of this progress has been achieved by developing finite-difference computer codes for solving the transonic small-disturbance (TSD) potential equation,[2] although significant efforts are currently underway at the higher equation levels as well. The advantages of the TSD formulation, especially for aeroelastic applications, are the relatively low computational cost and the simplicity of the gridding and geometry preprocessing. However, a serious limitation of the potential flow codes, in general, is the inability to predict accurately flows with strong shock waves. For these flows, use of the isentropic potential formulation typically results in shock waves that are too strong and located too far aft in comparison with the experiment. In fact, it is fairly well known that potential theory predicts nonunique steady-state solutions[3] for certain combinations of Mach number and angle of attack. Simple modifications to potential theory, however, have been shown to eliminate the nonuniqueness problem and, consequently, provide solutions that more accurately simulate those computed using the Euler equations.[4-7] These modifications include the effects of shock-generated entropy, and they require only minor changes to existing computer codes.

Rotational effects may also become important when strong shock waves are present in the flow. For example, vorticity is generated by shock waves due to the variation of entropy along the shock. Potential theory, of course, does not account for these effects because of the irrotationality assumption necessary for the existence of a velocity potential. For these flows, the Euler equations generally are required to model the flow accurately. Recently, however, simple modifications to potential theory have been developed to model rotational effects.[8-10] These modifications involve a velocity decomposition originally suggested by Clebsch.[11] In this model, the velocity vector is decomposed into a potential component and a rotational component. For most applications of interest to the aeroelastician, the rotational effects are significant only in the region downstream of shocks. Therefore, the potential component can be obtained throughout most of the flowfield using an existing potential flow code. The rotational flow then can be modeled either by adding the appropriate source term to the governing equation or by modifying the fluxes. These changes, consequently, include the effects of shock-generated vorticity as well as entropy, and require relatively straightforward modifications to existing potential flow codes.

Received Feb. 29, 1988; presented as Paper 88-2278 at the AIAA/ASME/ASCE/AHS 29th Structures, Structural Dynamics and Materials Conference, Williamsburg, VA, April 18-20, 1988; revision received Nov. 15, 1988.

*Research Scientist, Unsteady Aerodynamics Branch, Structural Dynamics Division. Senior Member AIAA.

The purpose of this paper is to present entropy and vorticity modifications to TSD theory, similar to the steady full-potential modifications of Refs. 8 and 10, for time-accurate applications. The modifications have been implemented in the computational aeroelasticity program-transonic small disturbance (CAP-TSD)[12] code that is capable of transonic aeroelastic analysis of complete aircraft configurations. The CAP-TSD code can be used to analyze configurations with arbitrary combinations of lifing surfaces and bodies including canard, wing, tail, control surfaces, tip launchers, pylons, fuselage, stores, and nacelles. The modified code models the effects of shock-generated entropy and vorticity while retaining the relative simplicity and cost efficiency of the TSD formulation. The paper presents detailed descriptions of the entropy and vorticity modifications, along with calculated results and comparisons with Euler solutions and with experimental data, which assess the present method.

Transonic Small-Disturbance Theory

The flow is assumed to be governed by the general-frequency TSD potential equation,[13] which may be written in conservation law form as

$$\frac{\partial f_0}{\partial t} + \frac{\partial f_1}{\partial x} + \frac{\partial f_2}{\partial y} + \frac{\partial f_3}{\partial z} = 0 \tag{1}$$

where

$$f_0 = -A\phi_t - B\phi_x \tag{2a}$$

$$f_1 = E\phi_x + F\phi_x^2 + G\phi_y^2 \tag{2b}$$

$$f_2 = \phi_y + H\phi_x\phi_y \tag{2c}$$

$$f_3 = \phi_z \tag{2d}$$

The coefficients A, B, and E are defined as

$$A = M^2 \qquad B = 2M^2 \qquad E = 1 - M^2 \tag{3}$$

Several choices are available for the coefficients F, G, and H depending on the assumptions used in deriving the TSD equation. The coefficients herein are defined as

$$F = -\tfrac{1}{2}(\gamma + 1)M^2 \tag{4a}$$

$$G = \tfrac{1}{2}(\gamma - 3)M^2 \tag{4b}$$

$$H = -(\gamma - 1)M^2 \tag{4c}$$

The lifting surfaces are modeled by imposing the following conditions:

Flow tangency:

$$\phi_z^{\pm} = f_x^{\pm} + f_t \tag{5a}$$

Trailing wake:

$$\Gamma_t + \Gamma_x = 0 \text{ and } \Delta\phi_z = 0 \tag{5b}$$

where $\Delta(\ )$ represents the jump in $(\ )$ across the wake. The flow-tangency condition is imposed along the mean plane of the respective lifting surface. In Eq. (5a), the plus and minus superscripts indicate the upper and lower surfaces of the mean plane, respectively. The wake is assumed to be a planar extension from the trailing edge to the downstream boundary of the finite-difference grid.

Entropy Model

Shock-generated entropy is modeled by implementing modifications to TSD theory similar to those reported in Refs. 6 and 7. These modifications include 1) an alternative streamwise flux, 2) an entropy correction in the pressure formula, and 3) a modified wake boundary condition to account for convection of entropy. In this section, the entropy model is briefly described. Additional details may be found in Refs. 6 and 7.

Alternative Streamwise Flux

The entropy model is formulated by first replacing the streamwise flux f_1 [Eq. (2b)] in the TSD equation by an alternative flux given by

$$f_1 = (\gamma + 1)M^2R(V\bar{V} - \tfrac{1}{2}V^2) + G\phi_y^2 \tag{6}$$

where

$$R = \left[\frac{2 + (\gamma - 1)M^2}{(\gamma + 1)M^2}\right]^{1/2} \tag{7a}$$

$$V = \frac{(1 + R)\phi_x}{1 + \phi_x + R} \tag{7b}$$

$$\bar{V} = \left(\frac{R^2 - 1}{2R}\right) \tag{7c}$$

The first term of this new flux was derived in Ref. 14 by an asymptotic expansion of the Euler equations including the effects of shock-generated entropy. The analysis of Ref. 14 shows that Eq. (6) is accurate to at least $0(\phi_x^3)$ in the expanded Euler equations. When ϕ_x is small, the alternative flux of Eq. (6) is the same as the original flux of Eq. (2b) to $0(\phi_x^2)$.

Pressure Correction

The pressure formula is modified to include entropy effects according to

$$C_p = C_{p_i} + C_{p_s} \tag{8}$$

where C_{p_i} is the isentropic pressure coefficient, and C_{p_s} is the pressure coefficient due to change in entropy. As reported in Refs. 6 and 7, C_{p_s} is given by

$$C_{p_s} = \frac{-2}{\gamma(\gamma - 1)M^2}\frac{s}{c_v} \tag{9}$$

Equation (9) obviously requires the determination of entropy along the surface of the airfoil or wing. This first requires the determination of the shock location and then the calculation of the entropy jump across the shock. The shock location is determined easily since most TSD algorithms use type-dependent differencing to capture shocks and to treat regions of subsonic and supersonic flow properly. The entropy jump is computed using the Rankine-Hugoniot shock jump relation

$$\frac{s}{c_v} = \ell n\frac{(\gamma + 1)u_1^2 - (\gamma - 1)R^2}{(\gamma + 1)R^2 - (\gamma - 1)u_1^2} - \gamma\ell n\frac{u_1^2}{R^2} \tag{10}$$

where

$$u_1 = 1 + \phi_x - u_s \tag{11}$$

In Eq. (11), u_1 is the flow speed upstream of the shock and u_s is the shock speed, which are computed at time level $(n + 1)$ to maintain time accuracy. In Refs. 6 and 7, the entropy was assumed to be constant between the shock and the trailing edge even for unsteady applications. In the present formulation, the entropy is convected downstream from the shock according to

$$\frac{\partial s}{\partial t} + \frac{\partial s}{\partial x} = 0 \tag{12}$$

The correction to the pressure formula to include entropy effects [Eq. (9)] does not directly effect the flowfield. The

effect on the flowfield is produced by the modified wake boundary condition discussed in the following section.

Modified Wake Boundary Condition

The wake boundary condition requires that the pressure be continuous across the wake. Since the pressure formula [Eq. (8)] includes a term due to entropy, the isentropic wake boundary condition must be modified as

$$\Gamma_t + \Gamma_x = \tfrac{1}{2}\Delta C_{p_s} \tag{13}$$

where Δ represents the jump across the wake. In Eq. (13), ΔC_{p_s} is determined by first convecting the entropy along the wake and then computing C_{p_s} using Eq. (9). The nonzero right-hand side of Eq. (13) modifies the circulation distribution Γ. Consequently, the circulation due to entropy opposes the circulation associated with lift and thus decreases the total circulation. As discussed in Ref. 6, this is the feedback mechanism that stabilizes the shock location and eliminates the nonuniqueness problem.

Vorticity Model

A vorticity model has been developed that is similar to that presented in Ref. 10. In this section, the vorticity model is described in detail including: 1) a modified velocity vector that in turn modifies the TSD equation, 2) a pressure formula correction for vorticity effects, and 3) the resulting wake boundary condition.

Modified Velocity Vector

The vorticity model is formulated by first writing the velocity vector as the sum of potential and rotational components according to

$$V = \nabla\Phi - \frac{1}{\gamma-1}\frac{s}{c_v}\nabla\Psi \tag{14}$$

In Eq. (14), the first term on the right-hand side is the gradient of a scalar potential Φ, and the second term involves the product of the entropy s and the gradient of a Clebsch variable Ψ. The function Ψ is a measure of the stretching and rotating of vortex filaments associated with entropy variation.[10] For the applications of interest in the present work, the rotational part of the velocity vector is assumed to occur only in the region downstream of the shock waves, as shown in Fig. 1. Further assuming that the entropy convects with the freestream speed [Eq. (12)] and that the shock curvature is negligible implies that

$$\frac{\partial\Psi}{\partial x} = \frac{1}{\gamma M^2}, \qquad \frac{\partial\Psi}{\partial y} = 0, \qquad \frac{\partial\Psi}{\partial z} = 0 \tag{15}$$

as shown in Ref. 10. These assumptions eliminate the variable Ψ from the formulation, leaving only the entropy s to be determined throughout the flowfield. In a steady flow, entropy is constant along streamlines and changes only through shock waves. The entropy jump is computed along shocks using the Rankine-Hugoniot relation [Eq. (10)]. Then, for simplicity, the grid lines are assumed to approximate the streamlines of the flow, which is consistent with the small-disturbance approximation. The entropy is either convected downstream along the grid lines using Eq. (12) for unsteady applications, or is held constant along the grid lines for steady applications.

The modified velocity vector in turn modifies the TSD equation because the streamwise disturbance speed $u = \phi_x$ is now given by

$$u = \phi_x - \frac{1}{\gamma(\gamma-1)M^2}\frac{s}{c_v} \tag{16}$$

The new TSD equation has the same conservation law form as Eq. (1), with new fluxes defined by simply replacing ϕ_x in Eq. (2) by the modified speed given in Eq. (16).

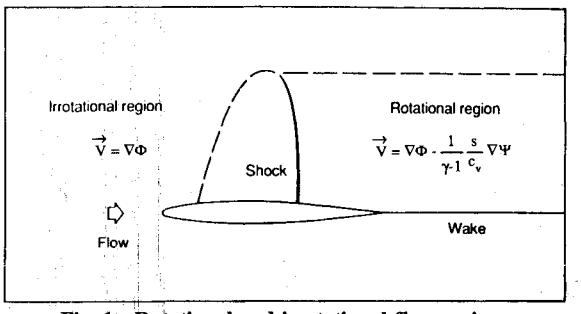

Fig. 1 Rotational and irrotational flow regions.

Pressure Correction

The pressure formula must also be modified when vorticity effects are included in the model. In general form, the pressure coefficient may be computed using

$$C_p = C_{p_i} + C_{p_s} + C_{p_v} \tag{17}$$

where C_{p_v} is the pressure coefficient correction due to vorticity. As discussed by Hafez and Lovell,[5] the correction due to vorticity approximately cancels the correction due to entropy and, thus, C_p is given by the isentropic formula. At the TSD equation level, this is clearly demonstrated by first considering the general form of Eq. (8). Assuming the first-order small-disturbance pressure formula for C_{p_t}, defining C_{p_s} as given by Eq. (9), and replacing ϕ_x by the modified disturbance speed of Eq. (16) yields

$$C_p = -2\phi_t - 2\phi_x - \frac{2}{\gamma(\gamma-1)M^2}\frac{s}{c_v} + \frac{2}{\gamma(\gamma-1)M^2}\frac{s}{c_v} \tag{18}$$

Here the corrections due to entropy and vorticity identically cancel each other and, thus, the pressure coefficient is given by the isentropic formula in terms of the irrotational disturbance speed ϕ_x.

Modified Wake Boundary Condition

As with the entropy model, the wake boundary condition in the vorticity model requires that the pressure be continuous across the wake. Since the pressure [Eq. (18)] is now given by the isentropic formula, the wake boundary condition is identical to the original condition given by

$$\Gamma_t + \Gamma_x = 0 \tag{19}$$

The feedback mechanism that eliminates the nonuniqueness problem is the rotational velocity field inherent in the vorticity model. This is in contrast to the mechanism of the entropy model, which is explicitly imposed through the wake boundary condition [Eq. (13)].

Approximate Factorization Algorithm

The approximate factorization (AF) algorithm of Ref. 15 has been modified to solve the TSD equation including entropy and vorticity effects. In this section, the AF algorithm is described.

General Description

The AF algorithm consists of a Newton linearization procedure coupled with an internal iteration technique. For unsteady flow calculations, the solution procedure involves two steps. First, a time linearization step (described in the following) is performed to determine an estimate of the potential field. Second, internal iterations are performed to minimize linearization and factorization errors. Specifically, the TSD equation (1) is written in general form as

$$R(\phi^{n+1}) = 0 \tag{20}$$

where ϕ^{n+1} represents the unknown potential field at time level $(n+1)$. The solution to Eq. (20) is then given by the Newton linearization of Eq. (20) about ϕ^*

$$R(\phi^*) + \left(\frac{\partial R}{\partial \phi}\right)_{\phi=\phi^*} \Delta\phi = 0 \tag{21}$$

In Eq. (21), ϕ^* is the currently available value of ϕ^{n+1} and $\Delta\phi = \phi^{n+1} - \phi^*$. During convergence of the iteration procedure, $\Delta\phi$ will approach zero so that the solution will be given by $\phi^{n+1} = \phi^*$. In general, only one or two iterations are required to achieve acceptable convergence. For steady flow calculations, iterations are not used since time accuracy is not necessary when marching to steady state.

Mathematical Formulation

The AF algorithm is formulated by first approximating the time derivative terms (ϕ_{tt} and ϕ_{xt}) by second-order-accurate finite-difference formulas. The TSD equation is rewritten by substituting $\phi = \phi^* + \Delta\phi$ and neglecting squares of derivatives of $\Delta\phi$, which is equivalent to applying Eq. (21) term by term. The resulting equation is then rearranged, and the left-hand side is approximately factored into a triple product of operators, yielding

$$L_\xi L_\eta L_\zeta \Delta\phi = -\sigma R(\phi^*, \phi^n, \phi^{n-1}, \phi^{n-2}) \tag{22}$$

where

$$L_\xi = 1 + \frac{3B}{4A}\xi_x \Delta t \frac{\partial}{\partial \xi} - \xi_x \frac{\Delta t^2}{2A} \frac{\partial}{\partial \xi} F_1 \frac{\partial}{\partial \xi} \tag{23a}$$

$$L_\eta = 1 - \xi_x \frac{\Delta t^2}{2A} \frac{\partial}{\partial \eta} F_2 \frac{\partial}{\partial \eta} \tag{23b}$$

$$L_\zeta = 1 - \xi_x \frac{\Delta t^2}{2A} \frac{\partial}{\partial \zeta} F_3 \frac{\partial}{\partial \zeta} \tag{23c}$$

The equations for the spatial fluxes F_1, F_2, F_3 and the residual R are given in Ref. 15. In Eq. (22), σ is a relaxation parameter that is normally set equal to 1.0. To accelerate convergence to steady state, the residual R may be overrelaxed using $\sigma > 1$. Equation (22) is solved using three sweeps through the grid by sequentially applying the operators L_ξ, L_η, and L_ζ as

$$\xi \text{ sweep: } L_\xi \Delta\bar{\phi} = -\sigma R \tag{24a}$$

$$\eta \text{ sweep: } L_\eta \Delta\bar{\bar{\phi}} = \Delta\bar{\phi} \tag{24b}$$

$$\zeta \text{ sweep: } L_\zeta \Delta\phi = \Delta\bar{\bar{\phi}} \tag{24c}$$

Further details of the algorithm development and solution procedure may be found in Refs. 15 and 16.

Time-Linearization Step

An initial estimate of the potentials at time level $(n+1)$ is required to start the iteration process. This estimate is provided by performing a time-linearization calculation. The equations governing the time-linearization step are derived in a similar fashion as the equations for iteration. The only difference is that the equations are formulated by linearizing about time level (n) instead of the iterate level $(*)$.

CAP-TSD Code

The AF algorithm has been used as the basis of the CAP-TSD code for transonic unsteady aerodynamic and aeroelastic analysis of realistic aircraft configurations. The code can be used to analyze configurations with arbitrary combinations of lifting surfaces and bodies including canard, wing, tail, control surfaces, tip launchers, pylons, fuselage, stores. and nacelles. The code has the option of half-span modeling for symmetric cases or full-span modeling to allow the treatment of antisymmetric mode shapes, fuselage yaw, or unsymmetric configurations such as an oblique wing or unsymmetric wing stores. Steady and unsteady pressures on several realistic aircraft configurations calculated using CAP-TSD, including comparisons with experimental data, are presented in Ref. 12. The calculated results are in good general agreement with the experimental pressure data, which validates CAP-TSD for multiple-component applications with mutual aerodynamic interference effects. Preliminary aeroelastic applications of CAP-TSD compare well with experimental data for subsonic, transonic, and supersonic freestream Mach numbers, which gives confidence in the code for aeroelastic prediction.[17,18]

Results and Discussion

To assess the entropy and vorticity modifications to TSD theory, results are presented for the NACA 0012 airfoil and the ONERA M6 wing.[19] The accuracy of these results is determined through detailed comparisons with Euler calculations and with available experimental data.

NACA 0012 Airfoil Results

For the NACA 0012 airfoil, calculations were performed on a grid that had 80 and 66 points in the streamwise and vertical directions, respectively. The grid extended 25 chord lengths above and below the airfoil and 20 chord lengths upstream and downstream of the airfoil. Four cases of increasing difficulty were selected to assess the modified theory systematically. The first two cases involve steady flow for nonlifting ($M = 0.84$, $\alpha_0 = 0$ deg) and lifting ($M = 0.8$, $\alpha_0 = 1.25$ deg) conditions. These results are compared with parallel Euler calculations. The third case is for the airfoil pitching harmonically about the quarter-chord with an amplitude of $\alpha_1 = 2.51$ deg and reduced frequency of $k = 0.0814$ at $M = 0.755$ and $\alpha_0 = 0.016$ deg. The calculations are compared with the experimental data of Ref. 20. This case is a challenging one for the modified TSD theory since the oscillating airfoil produces relatively large shock motions and the upper and lower surface shocks periodically appear and disappear during the cycle. The fourth case is for the airfoil pitching harmonically about the quarterchord with an oscillation amplitude of $\alpha_1 = 2.44$ deg and reduced frequency of $k = 0.081$ at $M = 0.599$ and $\alpha_0 = 4.86$ deg. These calculations also are compared with the data of Ref. 20. This case is also a very challenging one since the maximum angle of attack during a cycle of motion is 7.3 deg. This relatively large instantaneous angle of attack is normally considered to be outside the range of validity of TSD theory.

Nonlifting Steady Flow

Results are first presented for the NACA 0012 airfoil at $M = 0.84$ and $\alpha_0 = 0$ deg. This is the same case studied by Fuglsang and Williams[6] and by Whitlow et al.[21] At this Mach number and angle of attack, irrotational isentropic methods, either TSD or full-potential, predict nonunique solutions, as reported in Refs. 6 and 21, respectively. These nonunique or

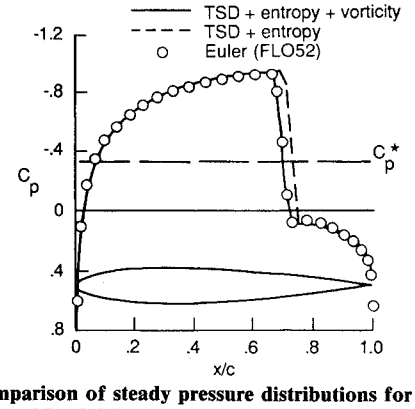

Fig. 2 Comparison of steady pressure distributions for the NACA 0012 airfoil at $M = 0.84$ and $\alpha_0 = 0$ deg.

multiple solutions are characterized by stable asymmetric flows with either large positive or large negative lift. The correct solution, of course, is a symmetric flow with zero lift. When shock-generated entropy effects are included in the calculation as a modification to the streamwise flux, the nonuniqueness problem is eliminated, and the expected symmetric solution is obtained, as shown in Fig. 2. The steady pressure distribution computed by including entropy effects compares fairly well with the Euler result,[14] except that the upper and lower surface shocks are located approximately 3% chord downstream of the Euler shock location. (For clarity, only every third pressure value from the Euler calculation was plotted except in the region of the shock.) This discrepancy in shock location is consistent with the entropy-corrected results for the same case shown in Refs. 6 and 21. When the shock-generated vorticity effects are also included in the model, however, the modified theory significantly improves the prediction of the shock location. Consequently, the steady pressure distribution now is in very good agreement with the Euler results, as further shown in Fig. 2. Therefore, for cases with strong shock waves, both entropy and vorticity corrections are required to give Euler-like accuracy.

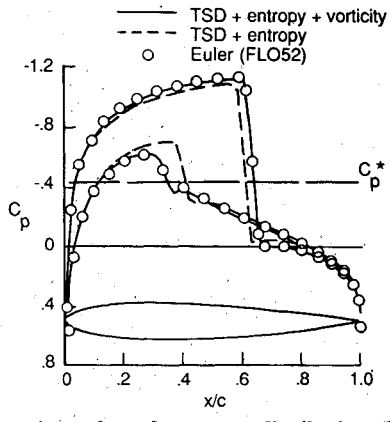

Fig. 3. Comparison of steady pressure distributions for the NACA 0012 airfoil at $M = 0.8$ and $\alpha_0 = 1.25$ deg.

Lifting Steady Flow

To evaluate the modified TSD method for a case with nonzero lift, results are presented for the NACA 0012 airfoil at $M = 0.8$ and $\alpha_0 = 1.25$ deg. This well-studied case is an AGARD test case for assessment of inviscid-flow methods.[22] Calculated pressures are presented in Fig. 3 for TSD theory

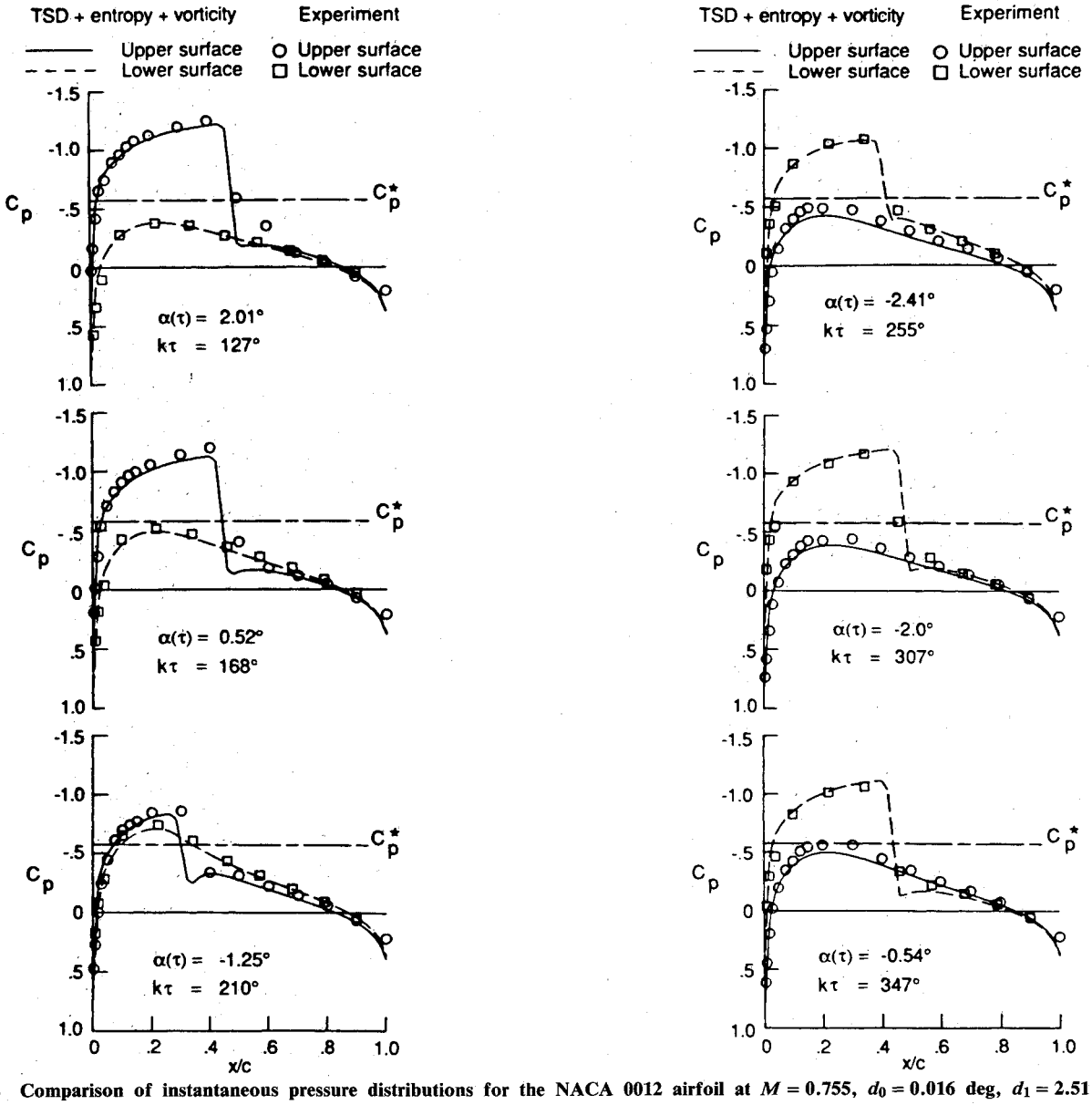

Fig. 4 Comparison of instantaneous pressure distributions for the NACA 0012 airfoil at $M = 0.755$, $d_0 = 0.016$ deg, $d_1 = 2.51$ deg, and $k = 0.0814$.

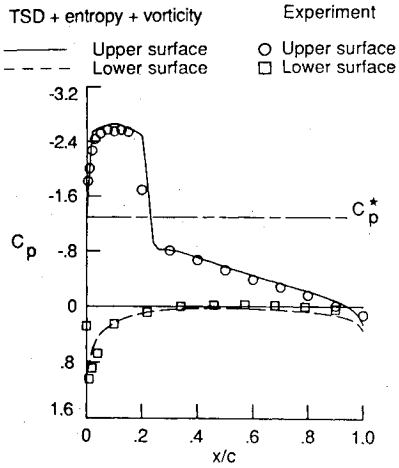

a) Near the maximum pitch angle, $\alpha(\tau) = 6.97$ deg, $k\tau = 60$ deg

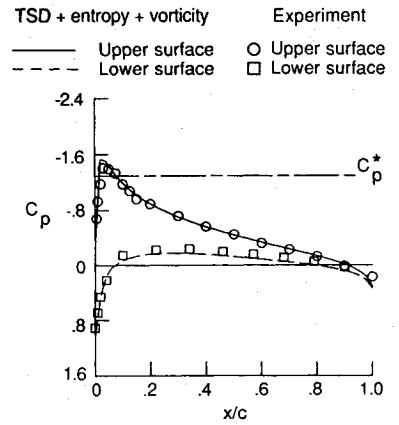

b) Near the minimum pitch angle, $\alpha(\tau) = 2.43$ deg, $k\tau = 273$ deg

Fig. 5. Comparison of instantaneous pressure distributions for the NACA 0012 airfoil at $M = 0.599$, $\alpha_0 = 4.86$ deg, $\alpha_1 = 2.44$ deg, and $k = 0.081$.

with entropy effects and TSD theory with entropy and vorticity effects. Comparisons are made with parallel Euler calculations to assess the accuracy of the TSD solutions. As shown in Fig. 3, the steady pressure distributions computed including entropy effects do not compare well with the Euler pressures. For example, the upper surface shock wave is slightly weaker and located approximately 3% chord upstream of the Euler result. Similarly, a stronger shock is predicted along the lower surface that is located about 6% chord downstream of the Euler calculation. When the vorticity effects are included in the calculation, however, the modified TSD theory gives steady pressures that are in very good agreement with the Euler results. Here, the strong shock on the upper surface and the weak shock on the lower surface are accurately predicted in both strength and location.

Unsteady Flows

To assess the modified theory for unsteady flow applications, results were first obtained for the NACA 0012 airfoil pitching harmonically about the quarterchord at $M = 0.755$ and $\alpha_0 = 0.016$ deg. This case was also studied in Ref. 21, where it was shown that the entropy effects have only a small effect on the solution. It is still a good check case, though, to test the robustness of the shock identification procedure and the smoothness of the entropy convection for a time-dependent problem with large shock motions. The amplitude of the motion was selected as $\alpha_1 = 2.51$ deg, and the reduced frequency was $k = 0.0814$ for comparison with the experimental data of Ref. 20. The results were obtained using 360 steps per cycle of motion, which corresponds to a step size of $\Delta t = 0.1072$. Three cycles of motion were computed to obtain a periodic solution.

Instantaneous pressure distributions at six points in time during the third cycle of motion are presented in Fig. 4 for comparison with the experimental pressure data. In each pressure plot, the instantaneous angle of attack $\alpha(\tau)$ and the angular position in the cycle are noted. During the first part of the cycle, there is a shock wave on the upper surface of the airfoil and the flow about the lower surface is predominantly subcritical. During the latter part of the cycle the flow about the upper surface is subcritical, and a shock forms along the lower surface. The pressure distributions from the modified theory indicate that the shocks oscillate over approximately 25% of the chord and, in general, compare well with the data. The modified theory captures the shocks sharply and has no difficulty in treating these large shock motions.

To assess further the modified theory for unsteady applications, pressures were calculated for the NACA 0012 airfoil pitching harmonically about the quarterchord at $M = 0.599$ and $\alpha_0 = 4.86$ deg. The amplitude of the motion was selected as $\alpha_1 = 2.44$ deg, and the reduced frequency was $k = 0.081$ for comparison with the experimental data.[20] The results were obtained using 360 steps per cycle of motion, and three cycles were computed to obtain a periodic solution.

Instantaneous pressure distributions at two points in time during the third cycle of motion are presented in Fig. 5. The two points in time correspond to near the maximum pitch angle ($\alpha = 6.97$ deg) shown in Fig. 5a, and near the minimum pitch angle ($\alpha = 2.43$ deg) shown in Fig. 5b. Near the maximum pitch angle (Fig. 5a), there is an imbedded supersonic region forward on the upper surface of the airfoil that is terminated by a relatively strong shock wave at approximately 20% chord. Instantaneous pressures obtained using the modified theory agree very well with the experimental data in the suction region $0.0 < x/c < 0.2$, and show accurate prediction of shock location and strength. The shock is sharply captured and is located slightly downstream of the experimental location. Near the minimum pitch angle (Fig. 5b), the shock wave on the upper surface disappears, and the calculated pressures again agree well with the data. The modified theory is, therefore, capable of treating time-dependent cases involving strong shocks and large shock motions.

ONERA M6 Wing Results

To test the entropy and vorticity modifications to TSD theory for three-dimensional applications, steady and unsteady calculations were performed for the ONERA M6 wing.[19] The M6 wing has an aspect ratio of 3.8, a leading-edge sweep angle of 30 deg, and a taper ratio of 0.562. The airfoil section of the wing is the ONERA "D" airfoil, which is a 10% maximum thickness-to-chord ratio symmetric section. Pressures were calculated at $M = 0.92$ with the wing at 0 deg mean angle of attack. These conditions correspond to an AGARD test case for assessment of inviscid flowfield methods,[22] and were selected for comparison with the tabulated Euler results of Rizzi contained therein. The calculations were performed on a grid that had 90, 30, and 60 points in the streamwise, spanwise, and vertical directions, respectively. The grid extended 10 root chord lengths upstream and downstream of the wing root, one semispan outboard of the wing tip, and 15 chord lengths above and below the wing.

Steady Flow

Calculations were performed for the ONERA M6 wing using: 1) unmodified TSD theory, 2) TSD with entropy effects, and 3) TSD with entropy and vorticity effects. For each of these methods, steady pressure distributions along three span stations ($\bar{\eta} = 0.08$, 0.47, and 0.82) of the wing are presented in Fig. 6. For this case, the flow is symmetric above and below the wing with shocks on the upper and lower surfaces. As shown in Fig. 6a, the results from the unmodified TSD theory compare well with the Euler results in predicting the leading-edge suction peak and the overall pressure levels. However, when compared with the Euler calculations, the shock is located too

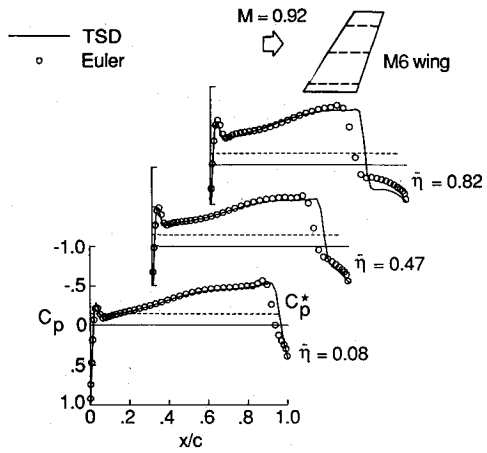

a) TSD

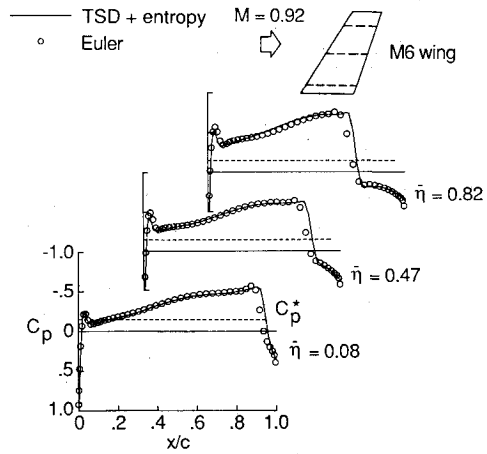

b) TSD + entropy

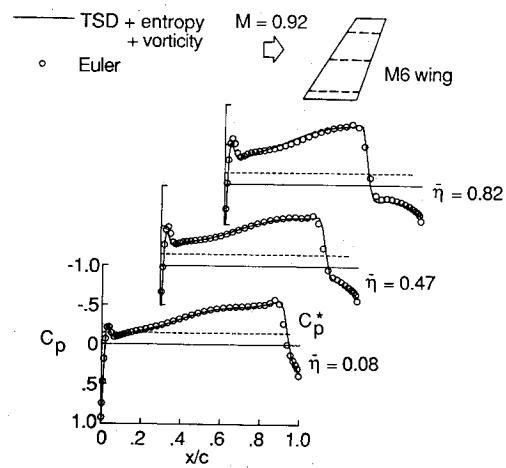

c) TSD + entropy + vorticity

Fig. 6. Comparison of steady pressure distributions for the ONERA M6 wing at $M = 0.92$ and $\alpha_0 = 0$ deg.

far aft and is too strong outboard near the tip. When the entropy effects are included in the calculation, a considerable improvement is obtained in both the shock location and strength, as shown in Fig. 6b. The shock is still located slightly downstream of the Euler shock position, along the span. When vorticity effects are also included in the calculation, the shock is displaced slightly forward from the previous solution, as shown in Fig. 6c. Here the shock location is in very good agreement with the Euler calculations along the span. Consequently, the steady pressure distributions from the modified TSD theory now compare very well with the Euler pressures, which verifies the modified theory for three-dimensional applications.

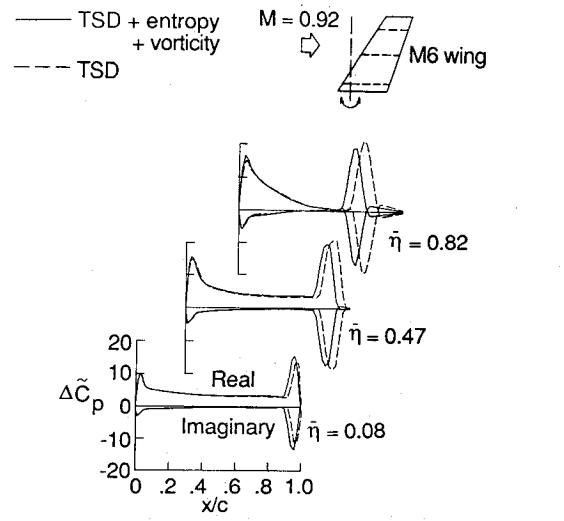

Fig. 7 Comparison of unsteady pressure distributions for the ONERA M6 wing at $M = 0.92$, $\alpha_0 = 0$ deg, $\alpha_1 = 2.51$ deg, and $k = 0.0814$.

Unsteady Flow

Unsteady results are also represented for the ONERA MG wing a $M = 0.92$ and $\alpha_0 = 0$ deg to demonstrate further application of the modified TSD theory to a time-dependent problem. Calculations were performed for the wing pitching harmonically about a line perpendicular to the root at the root quarter-chord. The amplitude of the motion was selected as $\alpha_1 = 2.51$ deg, and the reduced frequency was $k = 0.0814$, which are the same parameters as those used in the first of the unsteady cases for the NACA 0012 airfoil. The results were obtained using 360 steps per cycle of motion, which corresponds to a step size of $\Delta t = 0.1072$. Three cycles of motion were computed to obtain a periodic solution. There are no experimental unsteady data for the M6 wing to validate the calculated results.

Unsteady pressure distributions are shown in Fig. 7 for the same three span stations as the steady pressure distributions of Fig. 6. The results are presented as real and imaginary components of the unsteady lifting pressure coefficient, normalized by the amplitude of motion. Two sets of calculated pressures are compared corresponding to unmodified TSD theory and TSD with entropy and vorticity effects. As shown in Fig. 7, there is a shock pulse of moderate strength in both the real and imaginary parts that is produced by the motion of the shock wave. The shock pulse computed using the modified theory is located upstream of that predicted by the unmodified theory, corresponding to the forward displacement of the steady-state shock when the entropy and vorticity effects were included in the calculation (Fig. 6). In both cases shown in Fig. 7, the shock oscillates over 10–15% of the chord during a cycle of motion, and the modified theory has no difficulty in computing this unsteady transonic flow. Furthermore, differences between the two sets of results in Fig. 7 emphasize the importance of including the entropy and vorticity effects in the TSD calculation for unsteady aerodynamic and aeroelastic analysis. Preliminary applications of the modified TSD theory for aeroelastic analysis, including the effects of entropy and vorticity on flutter, have been reported in Ref. 23.

Concluding Remarks

Modifications to unsteady transonic small-disturbance theory to include entropy and vorticity effects were described. The modifications have been implemented in the CAP-TSD code, which was developed recently for aeroelastic analysis of complete aircraft configurations in the flutter critical transonic speed range. Entropy and vorticity effects have been incorporated within the solution procedure to treat cases with strong shock waves more accurately. The modified CAP-TSD code

includes these effects while retaining the relative simplicity and cost efficiency of the TSD formulation. For example, the entropy and vorticity corrections do not require any user-selected parameter values, and the increase in CPU time is only approximately 25%.

Steady and unsteady results were presented for the NACA 0012 airfoil and the ONERA M6 wing to demonstrate application of the modified theory. Comparisons were made with Euler calculations and with experimental data to assess the accuracy of the entropy and vorticity modifications. For the NACA 0012 airfoil, steady pressures computed using the modified theory were in very good agreement with the Euler calculations. For cases involving strong shock waves, both entropy and vorticity corrections were required to give Euler-like accuracy. Instantaneous pressure distributions obtained using the modified theory for the NACA 0012 airfoil pitching about the quarterchord compared well with experimental data. For the ONERA M6 wing, comparisons of steady pressures from the modified theory with Euler results also showed very good agreement. Therefore, the present method provides the aeroelastician with an affordable capability to analyze relatively difficult transonic flows without having to solve the computationally more expensive Euler equations.

References

[1]Edwards, J. W. and Thomas, J. L., "Computational Methods for Unsteady Transonic Flows," AIAA Paper 87-0107, Jan. 1987.

[2]Edwards, J. W., "Applications of Potential Theory Computations to Transonic Aeroelasticity," 15th International Council of the Aeronautical Sciences, Paper 86-2.9.1, Sept. 1986.

[3]Steinhoff, J. and Jameson, A., "Multiple Solutions of the Transonic Potential Flow Equation," AIAA Paper 81-1019, June 1981.

[4]Klopfer, G. H. and Nixon, D., "Nonisentropic Potential Formulation for Transonic Flows," *AIAA Journal,* Vol. 22, June 1984, pp. 770–776.

[5]Hafez, M. and Lovell, D. "Entropy and Vorticity Corrections for Transonic Flows," AIAA Paper 83-1926, July 1983.

[6]Fuglsang, D. F. and Williams, M. H., "Non-Isentropic Unsteady Transonic Small Disturbance Theory," AIAA Paper 85-0600, April 1985.

[7]Gibbons, M. D., Whitlow, W., Jr., and Williams, M. H., "Nonisentropic Unsteady Three Dimensional Small Disturbance Potential Theory," AIAA Paper 86-0863, May 1986.

[8]Grossman, B., "The Computation of Inviscid Rotational Gasdynamic Flows Using an Alternate Velocity Decomposition," AIAA Paper 83-1900, July 1983.

[9]Akay, H. U., Ecer, A., and Willhite, P. G., "Finite-Element Solutions of Euler Equations for Lifting Airfoils," *AIAA Journal,* Vol. 24, April 1986, pp. 562–569.

[10]Dang, T. Q. and Chen, L. T., "An Euler Correction Method for Two- and Three-Dimensional Transonic Flows," AIAA Paper 87-0522, Jan. 1987.

[11]Clebsch, A. "Uber die Integration der hydrodynamischen Gleichungen," *J. Reine Angew. Math.,* Vol. 57, 1859, pp. 1–10.

[12]Batina, J. T., Seidel, D. A., Bland, S. R., and Bennett, R. M., "Unsteady Transonic Flow Calculations for Realistic Aircraft Configurations," *Journal of Aircraft,* Vol. 26, Jan. 1989, pp. 21–28.

[13]Yoshihara, H., "Formulation of the Three-Dimensional Transonic Unsteady Aerodynamic Problem," Air Force Flight Dynamics Lab., Dayton, OH, AFFDL-TR-79-3030, Feb. 1979.

[14]Fuglsang, D. F., "Non-Isentropic Unsteady Transonic Small-Disturbance Theory," M. S. Thesis, Purdue Univ., West Lafayette, IN, May 1985.

[15]Batina, J. T., "Efficient Algorithm for Solution of the Unsteady Transonic Small-Disturbance Equation," *Journal of Aircraft*, Vol. 25, July 1988, pp. 598–605.

[16]Batina, J. T., "Unsteady Transonic Algorithm Improvements for Realistic Aircraft Applications," *Journal of Aircraft,* Vol. 26, Feb. 1989, pp. 131–139.

[17]Cunningham, H. J., Batina, J. T., and Bennett, R. M., "Modern Wing Flutter Analysis by Computational Fluid Dynamics Methods," *Journal of Aircraft,* Vol. 25, Oct. 1988, pp. 962–968.

[18]Bennett, R. M., Batina, J. T., and Cunningham, H. J., "Wing Flutter Calculations with the CAP-TSD Unsteady Transonic Small Disturbance Code," AIAA Paper 88-2347, April 1988.

[19]Schmitt, V. and Charpin, G., "Pressure Distributions on the ONERA M6 Wing at Transonic Mach Numbers," Appendix B1 in *Experimental Data Base for Computer Program Assessment,* AGARD-AR-138, May 1979.

[20]Landon, R. H., "NACA 0012. Oscillatory and Transient Pitching," Data Set 3 in *Compendium of Unsteady Aerodynamic Measurements,* AGARD-R-702, Aug. 1982.

[21]Whitlow, W., Jr., Hafez, M. M., and Osher, S. J., "An Entropy Correction Method for Unsteady Full Potential Flows with Strong Shocks," AIAA Paper 86-1768, June 1986.

[22]Yoshihara, H., "Test Cases for Inviscid Flow Field Methods," AGARD-AR-211, May 1985.

[23]Mohr, R. W., Batina, J. T., and Yang, T. Y., "Mach Number Effects on Transonic Aeroelastic Forces and Flutter Characteristics," AIAA Paper 88-2304, April 1988.